ACADÉMIE
DES SCIENCES
INSTITUT DE FRANCE

Comptes Rendus
Mécanique

Luc Dormieux and Eric Lemarchand

Some remarks concerning the propagation of edge cracks in fluid-saturated materials

Volume 354 (2026), p. 153-163

Online since: 10 March 2026

https://doi.org/10.5802/crmeca.351

The Comptes Rendus. Mécanique *are a member of the Mersenne Center for open scientific publishing*
www.centre-mersenne.org — e-ISSN : 1873-7234

ACADÉMIE DES SCIENCES
INSTITUT DE FRANCE

Comptes Rendus. Mécanique
2026, Vol. 354, p. 153-163
https://doi.org/10.5802/crmeca.351

Research article

Some remarks concerning the propagation of edge cracks in fluid-saturated materials

Luc Dormieux [a] **and Eric Lemarchand** [a]

[a] ENPC/UGE/CNRS/IPP, Laboratoire Navier, UMR 8205, Marne-la-Vallée, France

E-mails: luc.dormieux@enpc.fr, eric.lemarchand@enpc.fr

Abstract. The present work falls within the framework of linear fracture mechanics extended to saturated porous media. It aims at generalizing the classical crack propagation criteria by accounting for poromechanical coupling. The main objective is to identify the driving force of propagation which now depends on the pore pressure. The result is applied in particular to the two limit cases of drained and undrained regimes. It is shown on the example of the 3-points bending test that significantly different propagation thresholds can be obtained.

Keywords. Crack propagation criterion, driving force, porous media, poromechanical coupling, 3-points bending test.

Manuscript received 22 October 2025, revised 5 February 2026, accepted 13 February 2026, online since 10 March 2026.

1. Introduction

The classical theory of linear elastic fracture mechanics introduces the concepts of stress intensity factor and energy release rate in order to formulate the criterion of crack propagation. The present paper investigates some aspects of the extension of such a criterion in the case of a saturated porous material.

Important efforts have been made in the past to describe the poromechanical coupling in a saturated porous medium in the presence of cracks within the framework of poroelasticity (see e.g. [1,2]). In the present paper, emphasis is placed on irreversible evolutions: the main issue is the activation and the impact of the poromechanical coupling in the matter of loading-driven crack propagation, which should not be confused with the issue of fluid-driven crack propagation in a poroelastic medium (see e.g. [3]). Despite the interest of the issue of temperature change (see e.g. [4,5]), the present paper will however focus on the poromechanical coupling only. In other words, isothermal conditions are assumed, leaving the issue of temperature changes to a forthcoming publication.

The first task is to identify the driving force of crack propagation, which is expected to depart from its usual formulation in so far as it will depend on the pressure field. This first achievement will make it possible to generalize the criterion of propagation. The presence of the pore pressure in the expression of the driving force suggests to examine the two extreme cases on the scale of intensity of poromechanical coupling, namely the drained and the undrained regimes. In particular, we want to emphasize the fact that the thresholds that characterize the onset of propagation in each case might be significantly different in practice. The 3-points bending test performed on a saturated beam will be used as an example for illustrative purposes.

2. Fundamentals of continuum poromechanics and notations

Following the classical poromechanics terminology, it is first recalled that a thorough distinction has to be made between the terms solid and skeleton, each being associated to the same physical phase but to different geometric scales of description. The term *solid* is used at a refined scale at which solid and fluid phases occupy separate geometric domains (microscopic scale). In contrast, the terms *skeleton* or *solid skeleton* refer to the continuous description of the solid phase (macroscopic scale). At this latter scale, a fluid and a skeleton particles coexist at the same location, each possessing a specific geometric transformation. On the other hand, the terms *porous material* or *porous medium* refer to the superposition of the two particles or of the two continuous media, namely the fluid and the skeleton (see [6]).

Consider a representative elementary volume $\mathrm{d}V$ of fluid saturated porous material located at point $\boldsymbol{x}$ in the current configuration. Its initial configuration $\mathrm{d}V_0$ with respect to the geometric transformation of the skeleton is located at point $\boldsymbol{X}$. The displacement of the skeleton particle is defined by the vector $\boldsymbol{\xi} = \boldsymbol{x} - \boldsymbol{X}$. The linearized strain tensor $\boldsymbol{\varepsilon}$ in this transformation is the symmetric part of $\nabla\boldsymbol{\xi}$. The Cauchy stress tensor, also called total stress tensor is $\boldsymbol{\sigma}$ while the pore pressure is denoted by p. In the current (resp. initial) configuration $\mathrm{d}V$ (resp. $\mathrm{d}V_0$) of the r.e.v., the fluid saturated pore volume is $\phi\,\mathrm{d}V_0$ (resp. $\phi_0\,\mathrm{d}V_0$), where ϕ is referred to as the lagrangian porosity. The pore volume change in the geometric transformation of the skeleton from $\mathrm{d}V_0$ to $\mathrm{d}V$ is therefore $(\phi-\phi_0)\,\mathrm{d}V_0$. Under isothermal conditions, the fundamental thermodynamic identity of poroelasticity reads:

$$\dot{\psi} = \boldsymbol{\sigma} : \dot{\boldsymbol{\varepsilon}} + p\,\dot{\phi} \tag{1}$$

where ψ denotes the lagrangian volume density of free energy stored in the skeleton of the saturated porous material. This means that the elastic energy stored in the solid phase of the r.e.v. $\mathrm{d}V$ is $\psi\,\mathrm{d}V_0$. In order for the strain tensor and the pore pressure to play the role of thermodynamic state variables, it is convenient to introduce the auxiliary potential $\psi^* = \psi - p(\phi-\phi_0)$ with which the thermodynamic identity (1) reads (see [7]):

$$\dot{\psi}^* = \boldsymbol{\sigma} : \dot{\boldsymbol{\varepsilon}} - (\phi-\phi_0)\,\dot{p}. \tag{2}$$

The state equations of poroelasticity accordingly read:

$$\boldsymbol{\sigma} = \frac{\partial\psi^*}{\partial\boldsymbol{\varepsilon}}, \qquad \phi-\phi_0 = -\frac{\partial\psi^*}{\partial p}. \tag{3}$$

The linear poroelasticity framework is obtained when $\psi^*(\boldsymbol{\varepsilon}, p)$ is a quadratic potential:

$$\psi^* = \boldsymbol{\sigma}_0 : \boldsymbol{\varepsilon} + \frac{1}{2}\boldsymbol{\varepsilon} : \mathbb{C}_d : \boldsymbol{\varepsilon} - (p-p_0)\boldsymbol{B} : \boldsymbol{\varepsilon} - \frac{(p-p_0)^2}{2N} \tag{4}$$

which yields the linear state equations:

$$\boldsymbol{\sigma} = \boldsymbol{\sigma}_0 + \mathbb{C}_d : \boldsymbol{\varepsilon} - (p-p_0)\boldsymbol{B}, \qquad \phi-\phi_0 = \boldsymbol{B} : \boldsymbol{\varepsilon} + \frac{p-p_0}{N}, \tag{5}$$

where $\mathbb{C}_d$ is the so-called drained stiffness tensor, $\boldsymbol{B}$ is the Biot tensor and N is the first Biot modulus. The corresponding expression of the free energy reads:

$$\psi = (\boldsymbol{\sigma}_0 + \boldsymbol{B}p_0) : \boldsymbol{\varepsilon} + \frac{1}{2}\boldsymbol{\varepsilon} : \mathbb{C}_d : \boldsymbol{\varepsilon} + \frac{p^2-p_0^2}{2N}. \tag{6}$$

While $\phi-\phi_0$ quantifies the pore volume change, it is useful to introduce the corresponding fluid mass change. It is usually quantified by the lagrangian mass density m, such that $m\,\mathrm{d}V_0$ represents the change in fluid mass contained in the pore space of the r.e.v. It follows that

$m = \rho^f \phi - \rho_0^f \phi_0$. Under isothermal conditions, the mass density of the fluid ρ^f is in turn related to the pore pressure change by means of the fluid compression modulus K^f:

$$\frac{\mathrm{d}p}{K^f} = \frac{\mathrm{d}\rho^f}{\rho_0^f}.$$

In the linearized framework of poroelasticity, the second state equation of (5) can therefore be replaced by:

$$\frac{m}{\rho_0^f} = \boldsymbol{B} : \boldsymbol{\varepsilon} + \frac{p - p_0}{M}, \qquad \frac{1}{M} = \frac{1}{N} + \frac{\phi_0}{K^f}, \tag{7}$$

where M is the second Biot modulus. State equation (7) is particularly useful in the so-called undrained case where fluid mass transfer is prevented. In this situation, the pore pressure and the skeleton strain are related by $p - p_0 = -M\boldsymbol{B} : \boldsymbol{\varepsilon}$. Use of this relation in the first state equation of (5) yields:

$$\boldsymbol{\sigma} = \boldsymbol{\sigma}_0 + \mathbb{C}_u : \boldsymbol{\varepsilon}, \qquad \mathbb{C}_u = \mathbb{C}_d + M\boldsymbol{B} \otimes \boldsymbol{B}. \tag{8}$$

Hence, in undrained evolutions of the porous material, the latter behaves as a linear elastic material with the stiffness tensor $\mathbb{C}_u$ which is therefore known as *undrained* stiffness tensor.

3. The driving force of crack propagation in saturated porous media

The derivation of the driving force of crack propagation is usually presented under the assumption that the crack faces are free of stress. This however will hardly be a sufficiently general framework in the case of saturated porous media. In order to illustrate this point, let us consider the example of crack propagation in a 3-points bending experiment performed on a notched beam in which the loading actuator applies a given displacement at the mid-span of the beam. In the usual analysis, the pressure[1] acting on the crack is neglected. In the case of a fluid-saturated beam, the beam is immersed in a fluid reservoir at constant pressure p_0. The same fluid saturates the pore space. The initial pore pressure prior to bending is equal to the external reservoir pressure p_0. Therefore, unlike the dry case, the pressure p_0 acting on the crack faces cannot be neglected in the analysis. The theoretical framework that we look for must include this typical kind of loading.

The plane strain assumption is adopted. At any stage of the crack propagation process, the configuration of the porous structure is denoted by $\Omega(\ell)$ where ℓ denotes the current crack length. The boundary $\partial\Omega(\ell)$ comprises a constant part $\partial\Omega_0$ and the crack $\mathscr{F}(\ell)$. It is useful to introduce the "upper" and "lower" crack lips $\mathscr{F}^{\pm}(\ell)$ and the unit normal $\boldsymbol{N}$ oriented from $\mathscr{F}^+(\ell)$ towards $\mathscr{F}^-(\ell)$. Accordingly, we have:

$$\partial\Omega(\ell) = \partial\Omega_0 \cup \mathscr{F}^+(\ell) \cup \mathscr{F}^-(\ell).$$

The presence of a crack implies a possible discontinuity of the displacement field $\boldsymbol{\xi}$. The displacement field is $\boldsymbol{\xi}^{\pm}$ on $\mathscr{F}^{\pm}(\ell)$ and the displacement jump is $[\![\boldsymbol{\xi}]\!] = \boldsymbol{\xi}^+ - \boldsymbol{\xi}^-$. Hence, although the surfaces $\mathscr{F}^{\pm}(\ell)$ are geometrically superposed, they are mechanically distinct (see Figure 1). More precisely, we assume that each crack face is subjected to surface forces of the form $\boldsymbol{\Sigma} \cdot \boldsymbol{n}$, where $\boldsymbol{\Sigma}$ is a given symmetric tensor. The unit normal $\boldsymbol{n}$ to the crack face is $+\boldsymbol{N}$ on $\mathscr{F}^+(\ell)$, and $-\boldsymbol{N}$ on $\mathscr{F}^-(\ell)$. The important case of a uniform pressure p_0 acting on the crack faces, encountered in the above example of the 3-points bending experiment in saturated conditions, corresponds to $\boldsymbol{\Sigma} = -p_0\boldsymbol{\delta}$. Note that the model is relevant in the case of edge cracks where the pressure acting on the crack faces is controlled. While this study focuses on edge cracks, a detailed analysis dedicated to internal cracks can be found in [8].

[1] In the classical experimental setup, this is in general the air pressure.

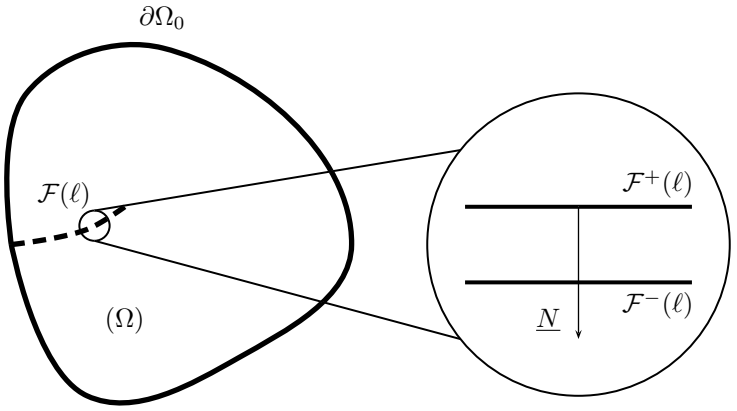

Figure 1. Domain Ω with crack $\mathscr{F}$. The principle of virtual work (25) includes a specific contribution of the crack.

In turn, the part $\partial\Omega_0$ of the boundary is split into two parts that are time independent:

$$\partial\Omega_0 = \partial\Omega_\xi \cup \partial\Omega_T.$$

Surface forces $\boldsymbol{T}^0(t)$ are prescribed on $\partial\Omega_T$ and displacements $\boldsymbol{\xi}^0(t)$ are prescribed on $\partial\Omega_\xi$. Body forces $\boldsymbol{F}(t)$ may also be considered. Eventually, in the general case, the mechanical loading $\mathscr{L}$ is defined by the tensor $\boldsymbol{\Sigma}$, the prescribed surface forces, displacements and body forces. For instance, in the 3-points bending experiment, the displacement is prescribed at the two supports and at the midspan. The surface forces on $\partial\Omega_T$ are constant and equal to $-p_0\boldsymbol{n}$. The crack faces are subjected to $\pm p_0\boldsymbol{N}$ ($\boldsymbol{\Sigma} = -p_0\boldsymbol{\delta}$).

Let us denote by Ψ the (lagrangian) free energy of the skeleton of the porous medium. In isothermal and quasistatic evolutions, the rate of dissipated energy $\mathscr{D}$ taking place in the skeleton, that is in the solid phase, during crack propagation reads:

$$\mathscr{D} = \mathscr{P}_e - \dot{\Psi} \geq 0.$$

In the above equation, $\mathscr{P}_e$ is the mechanical work provided to the skeleton. The expression of $\mathscr{P}_e$ reads:

$$\mathscr{P}_e = \int_{\Omega(\ell)} p\,\dot{\phi}\,\mathrm{d}V + \int_{\Omega(\ell)} \boldsymbol{F}\cdot\dot{\boldsymbol{\xi}}\,\mathrm{d}V + \int_{\partial\Omega_T} \boldsymbol{T}^0\cdot\dot{\boldsymbol{\xi}}\,\mathrm{d}S + \int_{\partial\Omega_\xi} \boldsymbol{T}\cdot\dot{\boldsymbol{\xi}}^0\,\mathrm{d}S + \int_{\mathscr{F}(\ell)} [\![\dot{\boldsymbol{\xi}}]\!]\cdot\boldsymbol{\Sigma}\cdot\boldsymbol{N}\,\mathrm{d}S. \qquad (9)$$

In the above expression, $\boldsymbol{T}$ denotes the surface force acting on $\partial\Omega_\xi$. It is recalled that the first term in (9) applies specifically to the saturated case. It is related to the work provided by the pore pressure applying to the internal solid walls of the porous material (see e.g. [2]). On the other hand, the last term is particular to the case of loaded crack faces. The rate $\dot{\phi}$ of porosity change and the velocity $\dot{\boldsymbol{\xi}}$ are the sum of the contribution of the crack propagation (under steady loading conditions and steady fluid mass density) and that of the loading and fluid mass density increment (under constant crack length):

$$\dot{\phi} = \frac{\partial\phi}{\partial\ell}_{|\mathscr{L}}\dot{\ell} + \dot{\phi}_{|\ell}, \qquad \dot{\boldsymbol{\xi}} = \frac{\partial\boldsymbol{\xi}}{\partial\ell}_{|\mathscr{L}}\dot{\ell} + \dot{\boldsymbol{\xi}}_{|\ell}, \qquad [\![\dot{\boldsymbol{\xi}}]\!] = \frac{\partial[\![\boldsymbol{\xi}]\!]}{\partial\ell}_{|\mathscr{L}}\dot{\ell} + [\![\dot{\boldsymbol{\xi}}]\!]_{|\ell}.$$

Accordingly, the mechanical power is split into two terms $\mathscr{P}_{e_{|\mathscr{L}}}$ and $\mathscr{P}_{e_{|\ell}}$. Under steady loading conditions, the mechanical power is due to crack propagation only:

$$\mathscr{P}_{e_{|\mathscr{L}}} = \left(\int_{\Omega(\ell)} p\,\frac{\partial\phi}{\partial\ell}_{|\mathscr{L}}\mathrm{d}V + \frac{\partial\Phi}{\partial\ell}_{|\mathscr{L}}\right)\dot{\ell}$$

with

$$\Phi = \int_{\Omega(\ell)} \boldsymbol{F}\cdot\boldsymbol{\xi}\,\mathrm{d}V + \int_{\partial\Omega_T} \boldsymbol{T}^0\cdot\boldsymbol{\xi}\,\mathrm{d}S + \int_{\mathscr{F}(\ell)} [\![\boldsymbol{\xi}]\!]\cdot\boldsymbol{\Sigma}\cdot\boldsymbol{N}\,\mathrm{d}S, \tag{10}$$

where Φ is the potential of the given loads (see Appendix A for mathematical details).

In turn, at constant crack length, we have:

$$\mathscr{P}_{e_{|\ell}} = \int_{\Omega(\ell)} p\,\dot{\phi}_{|\ell}\,\mathrm{d}V + \int_{\Omega(\ell)} \boldsymbol{F}\cdot\dot{\boldsymbol{\xi}}_{|\ell}\,\mathrm{d}V + \int_{\partial\Omega_T} \boldsymbol{T}^0\cdot\dot{\boldsymbol{\xi}}_{|\ell}\,\mathrm{d}S + \int_{\partial\Omega_\xi} \boldsymbol{T}\cdot\dot{\boldsymbol{\xi}}^0\,\mathrm{d}S + \int_{\mathscr{F}(\ell)} [\![\dot{\boldsymbol{\xi}}]\!]_{|\ell}\cdot\boldsymbol{\Sigma}\cdot\boldsymbol{N}\,\mathrm{d}S$$

and the principle of virtual work in its classical form readily yields:

$$\mathscr{P}_{e_{|\ell}} = \int_{\Omega(\ell)} p\,\dot{\phi}_{|\ell}\,\mathrm{d}V + \int_{\Omega(\ell)} \boldsymbol{\sigma} : \dot{\boldsymbol{\varepsilon}}_{|\ell}\,\mathrm{d}V.$$

Similarly, the free energy is the sum of two terms, namely $(\partial\Psi/\partial\ell)_{|\mathscr{L}}\dot{\ell}$ and $\dot{\Psi}_{|\ell}$, which correspond to the contributions of crack propagation and loading increment respectively:

$$\dot{\Psi} = \frac{\partial\Psi}{\partial\ell}_{|\mathscr{L}}\dot{\ell} + \dot{\Psi}_{|\ell}. \tag{11}$$

At constant crack length, no dissipation is produced. Therefore, we have:

$$\dot{\Psi}_{|\ell} = \mathscr{P}_{e_{|\ell}} = \int_{\Omega(\ell)} \left(\boldsymbol{\sigma} : \dot{\boldsymbol{\varepsilon}}_{|\ell} + p\,\dot{\phi}_{|\ell}\right)\mathrm{d}V. \tag{12}$$

The rate of dissipated energy eventually reads:

$$\mathscr{D} = \mathscr{P}_{e_{|\mathscr{L}}} - \frac{\partial\Psi}{\partial\ell}_{|\mathscr{L}}\dot{\ell} = G(\mathscr{L},\ell)\dot{\ell} \quad \text{with} \quad G(\mathscr{L},\ell) = \int_{\Omega(\ell)} p\,\frac{\partial\phi}{\partial\ell}_{|\mathscr{L}}\mathrm{d}V - \frac{\partial(\Psi-\Phi)}{\partial\ell}_{|\mathscr{L}}. \tag{13}$$

As opposed to the classical situation of a crack propagating in a non porous solid, the presence of a pressurized fluid in the pore space is responsible for an additional term in the expression of the driving force $G(\mathscr{L},\ell)$ of crack propagation. However, since the dissipation takes place in the solid phase of the porous material, it seems reasonable to resort to the same kind of criterion for crack propagation as in the case of a non porous solid (see e.g. [7]). Thus, introducing the critical energy G_c as a material constant of the porous material, such a criterion would take the form:

$$\begin{aligned} G(\mathscr{L},\ell) < G_c \quad &\Longrightarrow \quad \dot{\ell} = 0, \\ G(\mathscr{L},\ell) = G_c \quad &\Longrightarrow \quad \dot{\ell} \geq 0. \end{aligned} \tag{14}$$

Since G_c represents a dissipated energy that takes place in the solid phase, it is expected to depend on the skeleton only. This means that it should depend on the solid material together with geometrical properties of the microstructure of the solid phase. This also means that this material constant is believed to be affected neither by the poromechanical coupling nor by the fluid at stake.

4. The role of the poromechanical coupling on crack propagation: the 3-points bending experiment

For illustrative purposes of the above criterion (14), let us again consider the example of crack propagation in a 3-points bending experiment performed on a notched beam, in which the experiment is driven by the vertical displacement $\delta(t)$ of the point of force application. The initial crack length is ℓ_0.

As already stated, the experimental setup differs from the usual one in so far as the beam is immersed in a fluid reservoir at constant pressure p_0 (see Figure 2, right-hand side). Therefore,

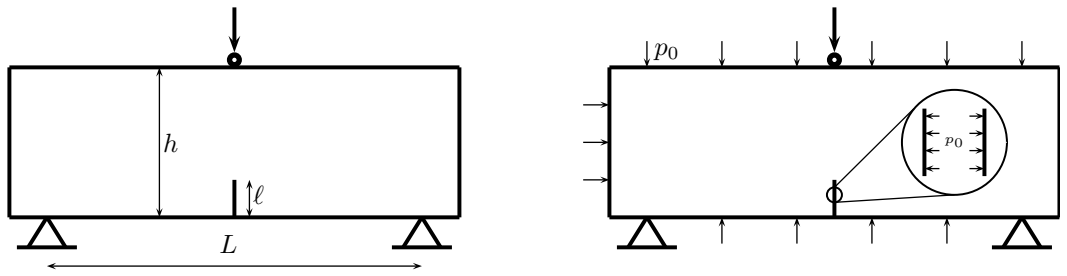

Figure 2. 3-points bend beam with edge crack subjected to concentrated load (left: dry experiment; right: saturated experiment).

while the crack propagates, its faces become subjected to the pressure p_0. As already stated, this situation is accounted for by setting $\boldsymbol{\Sigma} = -p_0\boldsymbol{\delta}$. Accordingly, the function Φ of (10) reads:

$$\begin{aligned}\Phi &= \int_{\partial\Omega_0} -p_0\boldsymbol{n}\cdot\boldsymbol{\xi}\,\mathrm{d}S + \int_{\mathscr{F}(\ell)} [\![\boldsymbol{\xi}]\!]\cdot\boldsymbol{\Sigma}\cdot\boldsymbol{N}\,\mathrm{d}S \\ &= \int_{\partial\Omega_0} -p_0\boldsymbol{n}\cdot\boldsymbol{\xi}\,\mathrm{d}S + \int_{\mathscr{F}^+(\ell)} -p_0\boldsymbol{N}\cdot\boldsymbol{\xi}^+\,\mathrm{d}S + \int_{\mathscr{F}^-(\ell)} +p_0\boldsymbol{N}\cdot\boldsymbol{\xi}^-\,\mathrm{d}S\end{aligned}$$

which means that:

$$\Phi = \int_{\partial\Omega(\ell)} -p_0\boldsymbol{n}\cdot\boldsymbol{\xi}\,\mathrm{d}S \tag{15}$$

where $\boldsymbol{n}$ is the unit normal vector to the external boundary. In particular, $\boldsymbol{n} = \pm\boldsymbol{N}$ on the crack faces $\mathscr{F}^{\pm}(\ell)$.

By definition, the initial stress field $\boldsymbol{\sigma}_0$ is in equilibrium with the pressure p_0 applied on the initial boundary $\partial\Omega_0 \cup \mathscr{F}^+(\ell_0) \cup \mathscr{F}^-(\ell_0)$:

$$\left(\partial\Omega_0 \cup \mathscr{F}^+(\ell_0) \cup \mathscr{F}^-(\ell_0)\right) \quad \boldsymbol{\sigma}_0\cdot\boldsymbol{n} = -p_0\boldsymbol{n}.$$

For further use, it will be convenient to note that (see (25)):

$$\int_{\Omega(\ell)} \boldsymbol{\sigma}_0 : \boldsymbol{\varepsilon}\,\mathrm{d}V = \int_{\partial\Omega_0} -p_0\boldsymbol{n}\cdot\boldsymbol{\xi}\,\mathrm{d}S + \int_{\mathscr{F}(\ell_0)} -p_0\boldsymbol{N}\cdot[\![\boldsymbol{\xi}]\!]\,\mathrm{d}S + \int_{\mathscr{F}(\ell)\setminus\mathscr{F}(\ell_0)} [\![\boldsymbol{\xi}]\!]\cdot\boldsymbol{\sigma}_0\cdot\boldsymbol{N}\,\mathrm{d}S.$$

The existence of a non homogeneous initial stress field refers to the issue of the effect of residual stresses on the crack propagation criterion. In order to focus on the role of poromechanical coupling, we further assume that the initial stress field is uniform, thus being equal to $-p_0\boldsymbol{\delta}$. In this case, the above equation yields:

$$\int_{\Omega(\ell)} \boldsymbol{\sigma}_0 : \boldsymbol{\varepsilon}\,\mathrm{d}V = \Phi.$$

This identity is in turn introduced into the expression (13) of the driving force, which now takes the form:

$$G(\mathscr{L},\ell) = \int_{\Omega(\ell)} p\,\frac{\partial\phi}{\partial\ell}_{|\mathscr{L}}\,\mathrm{d}V - \frac{\partial}{\partial\ell}\left(\int_{\Omega(\ell)} p_0\boldsymbol{B} : \boldsymbol{\varepsilon} + \frac{1}{2}\boldsymbol{\varepsilon} : \mathbb{C}_d : \boldsymbol{\varepsilon} + \frac{p^2 - p_0^2}{2N}\,\mathrm{d}V\right)_{|\mathscr{L}}. \tag{16}$$

In the above expression, it is recalled that the notation $_{|\mathscr{L}}$ stands for steady loading and steady fluid mass density conditions.

The analysis is conducted in the two extremal situations as regards the poromechanical coupling. In the ideal fully drained, the loading rate is sufficiently slow to ensure that the pore pressure does not change during bending. On the other hand, a fast loading rate prevents fluid mass transfer within the pore space, which in turn induces an undrained pore pressure change. Note that the expression (15) is valid under both drained and undrained conditions.

In view of forthcoming comparisons, it will prove useful to introduce the standard test which is performed on the same beam but in the absence of pore fluid and without any external pressure on the boundary of the beam. The stress and strain tensors $\boldsymbol{s}$ and $\boldsymbol{\varepsilon}$ are related by $\boldsymbol{s} = \mathbb{C}_d : \boldsymbol{\varepsilon}$. The loading is defined by the same displacement function $\delta(t)$. These loading conditions define the so-called reference dry problem, in which the function Φ is equal to 0 and the criterion of crack propagation involves the following driving force G_{dry}:

$$G_{\text{dry}} = -\frac{\partial}{\partial \ell}\left(\int_{\Omega(\ell)} \frac{1}{2}\boldsymbol{\varepsilon} : \mathbb{C}_d : \boldsymbol{\varepsilon}\, \mathrm{d}V\right)_{|\mathscr{L}}.$$

4.1. *The drained analysis*

Differentiating the state equations (5) with respect to ℓ at constant loading and fluid mass density, and then using the drained condition $p = p_0$, yields:

$$p\,\frac{\partial \phi}{\partial \ell}_{|\mathscr{L}} = p_0 \boldsymbol{B} : \frac{\partial \boldsymbol{\varepsilon}}{\partial \ell}_{|\mathscr{L}} + \frac{p_0}{N}\frac{\partial p}{\partial \ell}_{|\mathscr{L}} \tag{17}$$

and further[2]

$$\int_{\Omega(\ell)} p\,\frac{\partial \phi}{\partial \ell}_{|\mathscr{L}} \mathrm{d}V = \frac{\partial}{\partial \ell}\left(\int_{\Omega(\ell)} p_0 \boldsymbol{B} : \boldsymbol{\varepsilon} + \frac{p^2 - p_0^2}{2N}\,\mathrm{d}V\right)_{|\mathscr{L}}. \tag{18}$$

Introducing (18) into (16) yields

$$G(\mathscr{L}, \ell) = -\frac{\partial}{\partial \ell}\left(\int_{\Omega(\ell)} \frac{1}{2}\boldsymbol{\varepsilon} : \mathbb{C}_d : \boldsymbol{\varepsilon}\, \mathrm{d}V\right)_{|\mathscr{L}} \tag{19}$$

The pore pressure being uniform and steady ($p = p_0$), the first state equation (5) takes the form $\boldsymbol{\sigma} = -p_0\boldsymbol{\delta} + \mathbb{C}_d : \boldsymbol{\varepsilon}$. Owing to the respective boundary conditions of the present fully drained problem and of the reference dry problem (strain and stress fields $\boldsymbol{\varepsilon}$ and $\boldsymbol{s}$), it is readily seen that $\boldsymbol{\sigma} + p_0\boldsymbol{\delta} = \boldsymbol{s}$ and $\boldsymbol{\varepsilon} = \boldsymbol{\varepsilon}$. Eq. (19) can therefore be rewritten as:

$$G(\mathscr{L}, \ell) = -\frac{\partial}{\partial \ell}\left(\int_{\Omega(\ell)} \frac{1}{2}\boldsymbol{\varepsilon} : \mathbb{C}_d : \boldsymbol{\varepsilon}\, \mathrm{d}V\right)_{|\mathscr{L}} = -\frac{\partial}{\partial \ell}\left(\int_{\Omega(\ell)} \frac{1}{2}\boldsymbol{\varepsilon} : \mathbb{C}_d : \boldsymbol{\varepsilon}\, \mathrm{d}V\right)_{|\mathscr{L}} = G_{\text{dry}}. \tag{20}$$

Recalling the remark at the end of Section 3, this means that the crack propagation in fully drained conditions should follow the same law as in the dry case. More precisely, the onset of propagation is expected to occur at the same loading level.

4.2. *The undrained analysis*

The undrained analysis is a reasonable framework to provide a simplified physical analysis when the loading rate is high, thus preventing fluid mass transfer to take place. As already stated (see (8)), the porous material (as a whole) now behaves as a linear elastic material with stiffness $\mathbb{C}_u$. The pore pressure change is now directly related to the strain $\boldsymbol{\varepsilon}_u$ by (7):

$$p - p_0 = -M\boldsymbol{B} : \boldsymbol{\varepsilon}_u. \tag{21}$$

We then derive from (5) that:

$$p\,\frac{\partial \phi}{\partial \ell}_{|\mathscr{L}} = p\boldsymbol{B} : \frac{\partial \boldsymbol{\varepsilon}_u}{\partial \ell}_{|\mathscr{L}} + \frac{p}{N}\frac{\partial p}{\partial \ell}_{|\mathscr{L}}$$

and from (21):

$$p\,\frac{\partial \phi}{\partial \ell}_{|\mathscr{L}} = p_0 \boldsymbol{B} : \frac{\partial \boldsymbol{\varepsilon}_u}{\partial \ell}_{|\mathscr{L}} - \frac{\partial}{\partial \ell}\left(\frac{1}{2}\boldsymbol{\varepsilon}_u : M\boldsymbol{B}\otimes\boldsymbol{B} : \boldsymbol{\varepsilon}_u\right)_{|\mathscr{L}} + \frac{\partial}{\partial \ell}\left(\frac{p^2}{2N}\right)_{|\mathscr{L}}.$$

[2]Note that the order of implementation of the derivation operator $\frac{\partial}{\partial \ell}_{|\mathscr{L}}$ and integration operator $\int_{\Omega(\ell)}$ can be reversed. In contrast, as regards the integration operator $\int_{\partial\Omega(\ell)}$, a more precise insight is due (see Appendix A).

The above identity is finally introduced into (16):

$$G_u(\mathscr{L},\ell) = -\frac{\partial}{\partial \ell}\left(\int_{\Omega(\ell)} \frac{1}{2}\boldsymbol{\varepsilon}_u : \mathbb{C}_u : \boldsymbol{\varepsilon}_u \,\mathrm{d}V\right)_{|\mathscr{L}}. \tag{22}$$

As opposed to the dry case, or to the drained case, the expression of the driving force now involves the undrained stiffness tensor defined at (8). Furthermore, the strain field $\boldsymbol{\varepsilon}_u$ is now equal to the strain field $\boldsymbol{\varepsilon}_u$ that is encountered in dry conditions when the stiffness tensor is $\mathbb{C}_u$:

$$G_u(\mathscr{L},\ell) = -\frac{\partial}{\partial \ell}\left(\int_{\Omega(\ell)} \frac{1}{2}\boldsymbol{\varepsilon}_u : \mathbb{C}_u : \boldsymbol{\varepsilon}_u \,\mathrm{d}V\right)_{|\mathscr{L}}. \tag{23}$$

In other words, the undrained driving force is formally identical to the driving force *in the dry experiment*, except for the fact that the undrained stiffness tensor replaces the drained stiffness tensor.

5. Discussion and concluding remarks

As already stated, the main practical conclusion that can be drawn from (20) and (23) is that the driving forces of propagation respectively in drained and undrained conditions, for the same porous material and the same loading level (same value of the displacement δ) are in fact different. In each case, the driving force corresponds to the energy release rate in a specific dry experiment. In the drained case, the porous material should be replaced by a non porous material with stiffness tensor $\mathbb{C}_d$. In turn, in undrained conditions, the porous material should be replaced by a non porous material with stiffness tensor $\mathbb{C}_u$.

Let us now focus on the onset of propagation which is reached when the driving force is equal to the critical threshold G_c (see (14)). Let δ_d (resp. δ_u) denote the critical displacement that induces the onset of crack propagation in drained (resp. undrained) conditions, the initial length being ℓ_0. Accordingly, let q_α denote the corresponding line load thresholds ($\alpha = u, d$). With the notations and developments of Appendix B, it is found that:

$$-\frac{1}{2h}\mathscr{C}'_\alpha(\widetilde{\ell}_0)\delta_\alpha^2 = G_c \quad (\alpha = u, d).$$

From the proportionality rule (30), it can be concluded that

$$\delta_\alpha \propto \left(\frac{E_\alpha}{1-\nu_\alpha^2}\right)^{-1/2}, \qquad q_\alpha \propto \left(\frac{E_\alpha}{1-\nu_\alpha^2}\right)^{+1/2},$$

or

$$\frac{\delta_u}{\delta_d} = \frac{q_d}{q_u} = \sqrt{\frac{E_d}{E_u}\frac{1-\nu_u^2}{1-\nu_d^2}}.$$

This result highlights the fact that propagation thresholds, either in terms of displacement or forces, can be strongly dependent on the assumption concerning the fluid transfer that controls the intensity of the poromechanical coupling.

It should be noticed that the previous developments in the undrained regime are based on the assumption that the state equations (7) and (8) remain valid. In the case of a strong decrease of the pore pressure, this however becomes questionable if it reaches the threshold of the saturated vapour pressure. At this stage, a phase transition can take place and the fluid state equations must be reconsidered [8]. Still, the validity of the above conclusions is preserved if a metastable state takes place instead of a phase transition.

Declaration of interests

The authors do not work for, advise, own shares in, or receive funds from any organization that could benefit from this article, and have declared no affiliations other than their research organizations.

Appendix A.

Consider a stress field $\boldsymbol{\Sigma}$ meeting the momentum balance condition $\operatorname{div}\boldsymbol{\Sigma}=0$. The purpose of this section is to establish the identity:

$$\int_{\partial\Omega(\ell)}\frac{\partial}{\partial\ell}(\boldsymbol{\xi})\cdot\boldsymbol{\Sigma}\cdot\boldsymbol{n}\,\mathrm{d}S=\frac{\partial}{\partial\ell}\left(\int_{\partial\Omega(\ell)}\boldsymbol{\xi}\cdot\boldsymbol{\Sigma}\cdot\boldsymbol{n}\,\mathrm{d}S\right). \tag{24}$$

This result is used in the paper in the particular case of a uniform stress field $\boldsymbol{\Sigma}$.

To do so, let us first consider a domain Ω with external boundary $\partial\Omega_0$ (outwards oriented unit normal $\boldsymbol{n}$), comprising a crack $\mathscr{F}$. It is useful to introduce the "upper" and "lower" crack lips $\mathscr{F}^{\pm}$ and the unit normal $\boldsymbol{N}$ oriented from $\mathscr{F}^{+}$ towards $\mathscr{F}^{-}$. Accordingly, we have $\partial\Omega=\partial\Omega_0\cup\mathscr{F}^{+}\cup\mathscr{F}^{-}$.

Besides, the presence of a crack implies a possible discontinuity of the displacement field $\boldsymbol{\xi}$ which must be accounted for when applying the principle of virtual work. The displacement field is $\boldsymbol{\xi}^{\pm}$ on $\mathscr{F}^{\pm}$ and the displacement jump is $[\![\boldsymbol{\xi}]\!]=\boldsymbol{\xi}^{+}-\boldsymbol{\xi}^{-}$:

$$\int_{\Omega}\boldsymbol{\Sigma}:\mathbf{grad}\,\boldsymbol{\xi}\,\mathrm{d}V=\int_{\Omega}\boldsymbol{\Sigma}:\boldsymbol{\varepsilon}\,\mathrm{d}V=\int_{\partial\Omega_0}\boldsymbol{\xi}\cdot\boldsymbol{\Sigma}\cdot\boldsymbol{n}\,\mathrm{d}S+\int_{\mathscr{F}}[\![\boldsymbol{\xi}]\!]\cdot\boldsymbol{\Sigma}\cdot\boldsymbol{N}\,\mathrm{d}S. \tag{25}$$

The right-hand side in (24) is put in the incremental form:

$$\Delta=\frac{1}{\mathrm{d}\ell}\left(\int_{\partial\Omega(\ell+\mathrm{d}\ell)}\boldsymbol{\xi}(\ell+\mathrm{d}\ell)\cdot\boldsymbol{\Sigma}\cdot\boldsymbol{n}\,\mathrm{d}S-\int_{\partial\Omega(\ell)}\boldsymbol{\xi}(\ell)\cdot\boldsymbol{\Sigma}\cdot\boldsymbol{n}\,\mathrm{d}S\right).$$

Owing to the incremental propagation, it is convenient to split $\mathscr{F}(\ell+\mathrm{d}\ell)$ in the form:

$$\mathscr{F}(\ell+\mathrm{d}\ell)=\mathscr{F}(\ell)+\Gamma(\mathrm{d}\ell)$$

where $\Gamma(\mathrm{d}\ell)$ represents the crack increment of length $\mathrm{d}\ell$. Let us now use (25) twice. One obtains:

$$\int_{\partial\Omega(\ell)}\boldsymbol{\xi}(\ell)\cdot\boldsymbol{\Sigma}\cdot\boldsymbol{n}\,\mathrm{d}S=\int_{\Omega(\ell)}\boldsymbol{\Sigma}:\boldsymbol{\varepsilon}(\ell)\,\mathrm{d}V-\int_{\mathscr{F}(\ell)}[\![\boldsymbol{\xi}(\ell)]\!]\cdot\boldsymbol{\Sigma}\cdot\boldsymbol{N}\,\mathrm{d}S$$

as well as:

$$\int_{\partial\Omega(\ell+\mathrm{d}\ell)}\boldsymbol{\xi}(\ell+\mathrm{d}\ell)\cdot\boldsymbol{\Sigma}\cdot\boldsymbol{n}\,\mathrm{d}S=\int_{\Omega(\ell+\mathrm{d}\ell)}\boldsymbol{\Sigma}:\boldsymbol{\varepsilon}(\ell+\mathrm{d}\ell)\,\mathrm{d}V-\int_{\mathscr{F}(\ell+\mathrm{d}\ell)}[\![\boldsymbol{\xi}(\ell+\mathrm{d}\ell)]\!]\cdot\boldsymbol{\Sigma}\cdot\boldsymbol{N}\,\mathrm{d}S.$$

Let us now combine these two equations. First, we note that the volume integrals can be taken either on $\Omega(\ell)$ or on $\Omega(\ell+\mathrm{d}\ell)$. Indeed, the crack being a two-dimensional geometric object, its presence in the domains $\Omega(\ell)$ or $\Omega(\ell+\mathrm{d}\ell)$ does not affect the result of a volume integral. It follows, by difference, that:

$$\Delta=\int_{\Omega(\ell)}\boldsymbol{\Sigma}:\frac{1}{\mathrm{d}\ell}\big(\boldsymbol{\varepsilon}(\ell+\mathrm{d}\ell)-\boldsymbol{\varepsilon}(\ell)\big)\,\mathrm{d}V-\int_{\mathscr{F}(\ell)}\frac{1}{\mathrm{d}\ell}\Big([\![\boldsymbol{\xi}(\ell+\mathrm{d}\ell)]\!]-[\![\boldsymbol{\xi}(\ell)]\!]\Big)\cdot\boldsymbol{\Sigma}\cdot\boldsymbol{N}\,\mathrm{d}S$$
$$-\frac{1}{\mathrm{d}\ell}\int_{\Gamma(\mathrm{d}\ell)}[\![\boldsymbol{\xi}(\ell+\mathrm{d}\ell)]\!]\cdot\boldsymbol{\Sigma}\cdot\boldsymbol{N}\,\mathrm{d}S. \tag{26}$$

It remains to take the limit $\mathrm{d}\ell\to 0$ in the above equation. By definition of Δ, this yields:

$$\frac{\partial}{\partial\ell}\left(\int_{\partial\Omega(\ell)}\boldsymbol{\xi}\cdot\boldsymbol{\Sigma}\cdot\boldsymbol{n}\,\mathrm{d}S\right)=\int_{\Omega(\ell)}\boldsymbol{\Sigma}:\frac{\partial\boldsymbol{\varepsilon}}{\partial\ell}\,\mathrm{d}V-\int_{\mathscr{F}(\ell)}\frac{\partial[\![\boldsymbol{\xi}]\!]}{\partial\ell}\cdot\boldsymbol{\Sigma}\cdot\boldsymbol{N}\,\mathrm{d}S-\lim_{\mathrm{d}\ell\to 0}\left(\frac{1}{\mathrm{d}\ell}\int_{\Gamma(\mathrm{d}\ell)}[\![\boldsymbol{\xi}(\ell+\mathrm{d}\ell)]\!]\cdot\boldsymbol{\Sigma}\cdot\boldsymbol{N}\,\mathrm{d}S\right).$$

We have two things left to do. First, we have to notice that:

$$\frac{\partial}{\partial\ell}(\mathbf{grad}\,\boldsymbol{\xi})=\mathbf{grad}\left(\frac{\partial\boldsymbol{\xi}}{\partial\ell}\right),\qquad\frac{\partial[\![\boldsymbol{\xi}]\!]}{\partial\ell}=\left[\!\!\left[\frac{\partial\boldsymbol{\xi}}{\partial\ell}\right]\!\!\right].$$

The second remark refers to the order of magnitude of the displacement jump on $\Gamma(\mathrm{d}\ell)$, and namely that $\left|\left[\!\left[\boldsymbol{\xi}(\ell+\mathrm{d}\ell)\right]\!\right]\right| = \sqrt{\mathrm{d}\ell}$. This allows to conclude that:

$$\lim_{\mathrm{d}\ell\to 0}\left(\frac{1}{\mathrm{d}\ell}\int_{\Gamma(\mathrm{d}\ell)}\left[\!\left[\boldsymbol{\xi}(\ell+\mathrm{d}\ell)\right]\!\right]\cdot\boldsymbol{\Sigma}\cdot\boldsymbol{N}\,\mathrm{d}S\right)=0.$$

We have established that:

$$\frac{\partial}{\partial\ell}\left(\int_{\partial\Omega(\ell)}\boldsymbol{\xi}\cdot\boldsymbol{\Sigma}\cdot\boldsymbol{n}\,\mathrm{d}S\right)=\int_{\Omega(\ell)}\boldsymbol{\Sigma}:\mathbf{grad}\left(\frac{\partial\boldsymbol{\xi}}{\partial\ell}\right)\mathrm{d}V-\int_{\mathscr{F}(\ell)}\left[\!\left[\frac{\partial\boldsymbol{\xi}}{\partial\ell}\right]\!\right]\cdot\boldsymbol{\Sigma}\cdot\boldsymbol{N}\,\mathrm{d}S.$$

One last application of (25) with $\frac{\partial\boldsymbol{\xi}}{\partial\ell}$ instead of $\boldsymbol{\xi}$ in the right-hand side of the above equation eventually proves the validity of (24).

Appendix B.

Consider an isotropic linear elastic material (Young's modulus E, Poisson's ratio ν). The stress intensity factor in the dry 3-points bending experiment is given in [9] in the form (see Figure 2 for notations):

$$K=\sigma\sqrt{\pi\ell}\,g(\ell/h),\qquad \sigma=\frac{3L}{2h^2}q, \tag{27}$$

where q denotes the line load applied at the midspan in order to achieve the prescribed displacement δ. We introduce the dimensionless numbers $e=L/h$ and $\widetilde{\ell}=\ell/h$.

The ratio q/δ is a constant that can be interpreted as the effective stiffness coefficient of the structure $\mathscr{C}(\ell)$. In the dry experiment, the elastic energy W stored in the beam per unit length of thickness is $\frac{1}{2}q\delta$ and accordingly, the potential energy is $W_p=W=\frac{1}{2}\mathscr{C}(\widetilde{\ell})\delta^2$. Eventually, the energy release rate $-\partial W_p/\partial\ell$ is $-\frac{1}{2h}\mathscr{C}'(\widetilde{\ell})\delta^2$ and is related to the stress intensity factor by Irwin's formula (plane strain conditions):

$$-\frac{\partial W_p}{\partial\ell}=-\frac{1}{2h}\mathscr{C}'(\widetilde{\ell})\delta^2=\frac{1-\nu^2}{E}K^2$$

which can be put in the form:

$$\frac{\mathrm{d}}{\mathrm{d}\widetilde{\ell}}\left(\frac{1}{\mathscr{C}}\right)=\lambda\frac{1-\nu^2}{E}\gamma(\widetilde{\ell})$$

with $\lambda=\frac{9\pi}{2}e^2$ and $\gamma(\widetilde{\ell})=\widetilde{\ell}\,g^2(\widetilde{\ell})$. Then, by integration with respect to $\widetilde{\ell}$:

$$\frac{1}{\mathscr{C}(\widetilde{\ell})}=\frac{1}{\mathscr{C}(\widetilde{\ell}_0)}+\lambda\frac{1-\nu^2}{E}\int_{\widetilde{\ell}_0}^{\widetilde{\ell}}\gamma(\alpha)\,\mathrm{d}\alpha \tag{28}$$

where $\widetilde{\ell}_0$ corresponds to any reference length. Interestingly, in the limit case $\widetilde{\ell}_0\to 0$, the elastic compliance $1/\mathscr{C}(0)$ can be approximated by the one dimensional theory of elastic beams, provided that the slenderness ratio e is high enough. Under plain strain conditions, it is found that:

$$e\gg 1\quad\Longrightarrow\quad\lim_{\widetilde{\ell}_0\to 0}1/\mathscr{C}(\widetilde{\ell}_0)=1/\mathscr{C}_{1D}=\frac{1-\nu^2}{E}\frac{e^3}{4}. \tag{29}$$

In this framework, it can be concluded (from (29) together with (28)) that the effective stiffness coefficients $\mathscr{C}(0)$ and $\mathscr{C}(\widetilde{\ell})$ are proportional to $E/(1-\nu^2)$. This conclusion also applies to the energy release rate.

As expected, when the slenderness ratio decreases, the above approximation (29) of the elastic compliance $1/\mathscr{C}(0)$ becomes inaccurate. However, as shown in Figure 3, the ratio $\mathscr{C}_{1D}/\mathscr{C}(0)$ proves to remain almost independent of the Poisson's ratio. This implies that the proportionality rule of $\mathscr{C}(0)$ and $\mathscr{C}(\widetilde{\ell})$ with respect to $E/(1-\nu^2)$ still remains essentially valid:

$$\mathscr{C}(\widetilde{\ell})\propto\frac{E}{1-\nu^2}. \tag{30}$$

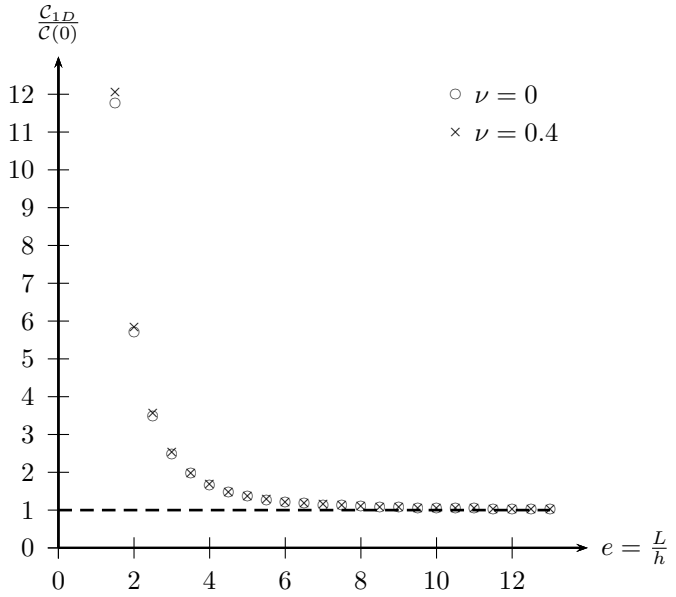

Figure 3. 3-points bending test: comparison of the numerical estimate by FEM of the compliance $\mathscr{C}(0)$ with the one-dimensional estimate as a function of the slenderness ratio e for two different values of the Poisson's ratio ($\nu = 0$ and $\nu = 0.4$).

References

[1] R. V. Craster and C. Atkinson, "Crack problems in a poroelastic medium: an asymptotic approach", *Philos. Trans. R. Soc. Lond., Ser. A* **346** (1994), no. 1680, pp. 387–428.

[2] L. Dormieux, D. Kondo and F.-J. Ulm, *Microporomechanics*, John Wiley & Sons, 2006.

[3] E. A. Bergkamp, C. V. Verhoosel, J. J. C. Remmers and D. M. J. Smeulders, "A thermodynamically consistent J-integral formulation for fluid-driven fracture propagation in poroelastic continua", *J. Mech. Phys. Solids* **170** (2023), article no. 105082 (29 pages).

[4] H. D. Bui, A. Ehrlacher and Q. S. Nguyen, "Propagation de fissure en thermoélasticité dynamique", *J. Méc., Paris* **19** (1980), no. 4, pp. 697–723.

[5] H. D. Bui, A. Ehrlacher and Q. S. Nguyen, "Étude expérimentale de la dissipation dans la propagation de fissure par thermographie infra-rouge", *C. R. Acad. Sci. Paris* **293** (1981), pp. 1015–1018.

[6] O. Coussy, *Mechanics of porous continua*, John Wiley & Sons, 1995.

[7] L. Dormieux and D. Kondo, *Micromechanics of fracture and damage*, Micromechanics Set, vol. 1, ISTE; John Wiley & Sons, 2016.

[8] L. Dormieux, E. Lemarchand, T. Carlioz and L. Jeannin, "Crack nucleation in saturated porous media", *Int. J. Numer. Anal. Methods Geomech.* **44** (2020), no. 5, pp. 553–574.

[9] S. Shah, S. Swartz and C. Ouyang, *Fracture mechanics of concrete*, John Wiley & Sons, 1995.